Hindawi
Advances in Polymer Technology
Volume 2020, Article ID 6714097, 10 pages
https://doi.org/10.1155/2020/6714097

Research Article

Ductile to Brittle Transition of Short Carbon Fiber-Reinforced Polypropylene Composites

Harri Junaedi,[1] **Essam Albahkali**,[1] **Muneer Baig**,[2] **Abdulsattar Dawood**,[3] **and Abdulhakim Almajid**[1,2]

[1]*Department of Mechanical Engineering, College of Engineering, King Saud University, P.O. Box 800, Riyadh 11421, Saudi Arabia*
[2]*Department of Engineering Management, College of Engineering, Prince Sultan University, P.O. Box 66833, Riyadh 11586, Saudi Arabia*
[3]*Saudi Arabian Basic Industries Corporation (SABIC), Riyadh, Saudi Arabia*

Correspondence should be addressed to Harri Junaedi; hjunaedi@ksu.edu.sa

Received 8 July 2020; Revised 18 October 2020; Accepted 26 October 2020; Published 5 November 2020

Academic Editor: Sagar Roy

In this work, the ductile to brittle transition behavior of short carbon fiber (SCF)-reinforced polypropylene (PP) composite is studied. Initially, the SCF-reinforced PP composites with a varying composition of SCF in the range of 0–40 wt% loading were first melt-mixed in a twin-screw extruder and later injection-molded to produce the testing samples. The experimental results indicate that with an increase in SCF loading, an increase in the tensile modulus and strength was observed along with a rapid decrease in the values of strain at break. A sudden decrease in strain at break was observed in composites in the range of 10–15 wt% SCF. To further study the sudden decrease in strain at break, an investigation was performed on composites that contained 10–15 wt% of SCF loading, starting from 10 wt% with a 1% increment to 15 wt% of SCF. The results of this study show that a decrease in strain at break was not linear; on the contrary, it was accompanied by a ductile to brittle transition, which specifically occurred in the range of 12–13 wt% of SCF loading and then continued to decrease with an increase in SCF loading.

1. Introduction

Polypropylene (PP) has been used in the automotive industry primarily in interior and exterior parts [1]. The use of PP in automotive industry increased over the years. PP is often used in the form of composites, as either fiber- or filler-reinforced composites. Short carbon fiber-reinforced PP composite is a widely used composite. Although studies on PP/short carbon fiber (SCF) composites have been conducted for many years, interesting results on this composite system are still being obtained. Short fiber-reinforced thermoplastics are very popular composites owing to the ease of processability, light weight, and recyclability [2–5]. Recently [3], the application of recycled carbon fibers has become possible, which can decrease the carbon fiber costs by up to 70% compared to the use of virgin fibers. The use of carbon fibers as filler materials in composites is attributed to the properties of carbon fibers such as high strength, high stiffness, low density (1.75–2.00 g/cm^3), chemical resistance, thermal stability, and high electrical and heat conductivity. Carbon fibers are mainly used as reinforcement on composite materials. Carbon fibers are usually used in the form of continuous and short fibers. The term "short" in the short fiber is defined as fiber whose length is on the order of 100 times its diameter. If the aspect ratio of length to diameter is within 100, then, the fiber is called a short fiber [6]. SCFs are available as chopped and milled fibers [7]. Chopped carbon fibers usually consist of bundled fibers, while milled fibers are usually powders. Milled carbon fibers tend to be easier to process with conventional extruder compared to chopped carbon fibers.

In general, a thermoplastic polymeric material at ambient temperature has low strength, low modulus, and high ductility. On the other hand, carbon fiber possesses high strength and high modulus and is very brittle. The combination of

thermoplastic polymer with carbon fibers will produce a composite material whose properties are between those of the precursor. The properties of thermoplastic-SCF composite somewhat depend on the properties of the precursor. The properties of composites are also affected by many factors. Some of the factors affecting the composite properties are the type of thermoplastic polymer, fiber loading, fiber length, quality dispersion of the fiber, fiber orientation, fiber size, compatibilizer, and processing conditions [8–11]. Processing route affects the composite properties. In injection-molded composites, the composite tends to have high ductility, and fibers are oriented in the injection direction. In hot compression molding, composites tend to have lower ductility and a more random orientation compared to injection molding [12–17]. The use of compatibilizer enhances the bonding between fibers and polymer and increases the interfacial strength of the precursor [18]. In general, the addition of SCFs into the thermoplastic matrix increases the tensile strength and modulus of elasticity of the composites. The ductility and toughness of the composites exhibit an opposite trend; specifically, ductility and toughness decrease with the addition of SCFs [19].

A decrease in strain at break (ductility) is one of the major drawbacks in SCF-reinforced thermoplastic composites. This drawback reduces the possible application of the composites. Most of the studies, which have been conducted on this composite system, focus on the effect of fibers on elasticity modulus and tensile strength. Fewer studies focus on the ductility and toughness performance of the composites. In most studies, strain at break has been reported to gradually decrease with the addition of SCF. Linear curve fitting for the strain at break was usually assumed. However, many studies have shown that the decrease in ductility is not gradual and there is always a considerable decrease in the ductility of composite at certain percentages of SCF [8, 9, 18]. At a certain percentage of filler, a transition from ductile to brittle occurs. This behavior was not investigated in detail because the focus of most studies was mostly on improving the strength and modulus. Understanding the behavior of strain at break of the composite is essential to have proper design and application of the composites.

The objective of this study is to investigate the effect of fiber content on the performance of SCF-reinforced PP composites. A thorough investigation of ductility as a function of filler content is performed. In this study, tensile tests were performed on reinforced PP composites. The tensile strength, modulus of elasticity, and strain at break were investigated. The microstructures of the composites were observed by an optical microscopy to understand the mechanism of mechanical behavior of the composites. Fracture surfaces of the composites were examined by scanning electron microscopy (SEM) to understand the fracture behavior.

2. Materials and Methods

2.1. Materials. The materials used in this study are isotactic polypropylene (iPP) polymer and SCF. iPP used was obtained from SABIC company in the form of particulates with a standard melt flow index (MFI) of 3.1 g/10 min. The MFI was measured at a temperature of 230°C and load of 2.16 kg. SCF was obtained from Asbury Carbons; SCF was the AGM94 grade milled carbon fiber with a diameter of 7–9 μm and an average length of 150 μm. The initial properties of PP and SCF are shown in Tables 1 and 2, respectively.

Table 1: Properties of polypropylene (data from the manufacturer).

Properties	Unit	Value
Melt flow rate	g/10 min	3.1
Density	kg/m^3	905
Tensile strength (at 50 mm/min speed)	MPa	37
Strain at yield (at 50 mm/min speed)	%	10
Tensile modulus (at 1 mm/min speed)	MPa	1550
Notched Izod impact strength at 23°C	kJ/m^2	3.5

Table 2: Properties of SCF (data from the manufacturer).

Properties	Unit	Value
Grade	—	AGM94
Type	—	Pitch
Fiber diameter	Microns	7–9
Density	g/cc	1.73–1.79
Carbon	%	94
Tensile strength	GPa	2–3.8
Young's modulus	GPa	180–240

Table 3: Composition of composites containing 5–40 wt% of SCF.

Tag name	wt% SCF
Neat PP	0
PP/5SCF	5
PP/10SCF	10
PP/15SCF	15
PP/20SCF	20
PP/30SCF	30
PP/40SCF	40

2.2. Processing. The PP-reinforced composites used in this study were processed by incorporating varying percentages of SCF. The concentration of SCF in the composites varied from 0 wt% of SCF, representing pure (neat) PP, to the maximum of 40 wt% of SCF. Table 3 shows the different compositions of the composites considered in this study. Altogether, six different combinations of the composites were prepared in addition to neat PP. Initially, PP and the desired percent of SCF were dry-mixed by a mechanical mixer to disperse SCF in PP. The mixed materials were later melt-mixed in a twin-screw extruder at the processing temperature of 210°C to form composite pellets. These pellets were used to produce the tensile test specimens using an injection molding machine operating at 230°C.

2.3. Characterization of Composites. Uniaxial tensile experiments were performed on the composites according to

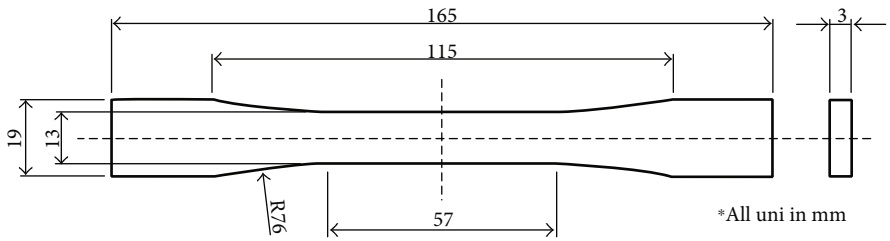

Figure 1: Dimensions of the tensile test specimen (ASTM D638 type I).

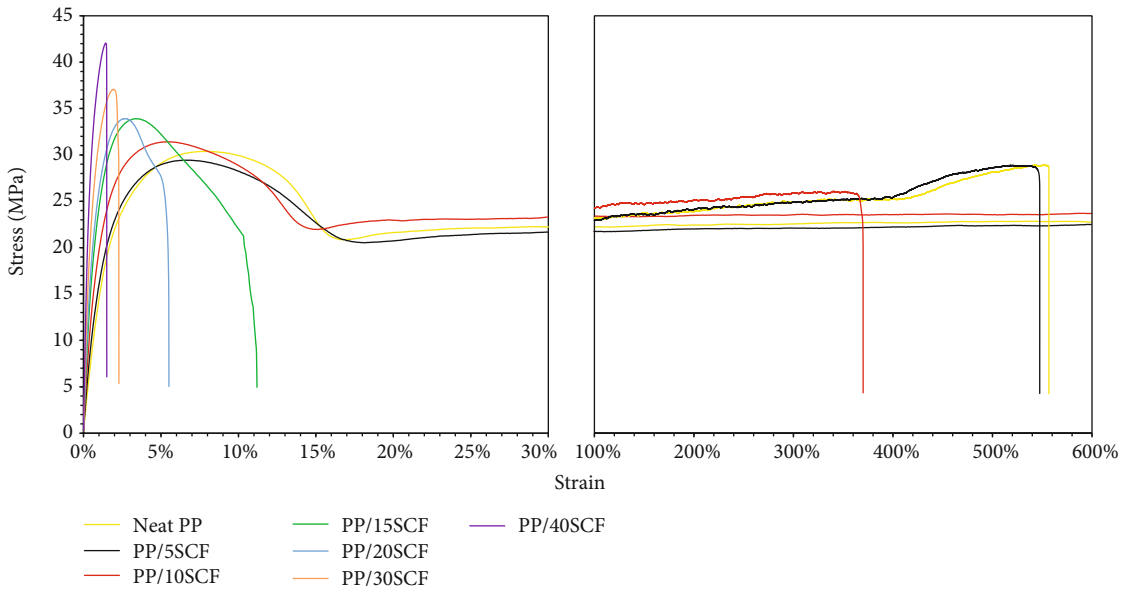

Figure 2: Representative stress-strain diagram of PP/SCF composites with 0–40 wt% of SCF.

ASTM D638-14 with type I sample [20] to measure their ultimate tensile strength (UTS), modulus of elasticity, and strain at break. The dimension of the sample is shown in Figure 1. These experiments were performed at room temperature on an Instron Universal Testing Machine, operating with the cross-head speed of 5 mm/min. An extensometer was used to measure the strain in the elastic regime and later to calculate the modulus of elasticity. To obtain a considerable amount of statistical data, at least three tensile samples were used for each composition mentioned in Table 3. An Olympus optical microscope was used to observe the microstructure of the composites. The fracture surface of tensile samples was analyzed using SEM (JSM-6610 LV).

Table 4: Mechanical properties of neat PP and its composites with 0–40 wt% of SCF.

Tag name	Modulus of elasticity (MPa)	Ultimate tensile strength (UTS) (MPa)	Strain at break (%)
Neat PP	1643 ± 45	30 ± 0.6	553 ± 38.5
PP/5SCF	2144 ± 36	29.6 ± 0.2	556 ± 12.5
PP/10SCF	3033 ± 54.4	31.4 ± 0.3	379 ± 48
PP/15SCF	4333 ± 183	33.7 ± 0.3	12 ± 2.5
PP/20SCF	5294 ± 373	33.6 ± 0.6	5.4 ± 0.3
PP/30SCF	8022 ± 232	37.4 ± 0.5	2.2 ± 0.2
PP/40SCF	11088 ± 281	42.2 ± 0.2	1.5 ± 0.2

3. Results and Discussion

3.1. Mechanical Properties. Figure 2 shows the stress-strain curves for neat PP and PP/SCF composites. The experimental results show that up to the addition of 10 wt% of SCF, the stress-strain curve reaches the maximum stress value, after which necking starts to form. The formation of necking leads to a gradual decrease in stress values, which creates a hump, followed by a near-horizontal curve. The near-horizontal part of the curve is the condition where PP molecular chains tend to align in the direction of elongation or load [21]. For the composite samples with 10 wt% of SCF, the strain at break can reach up to the value of 379%, while for the SCF content of 15 wt% and higher, the samples broke at an approximately 12% strain. This occurs owing to the considerable amount of SCF loading in the composite; thus, the molecular chain alignment process is hindered. This assumption can be justified by the fact that the alignment of the matrix molecule chain can be only possible when there exists matrix continuity. The excessive presence of SCF in the PP

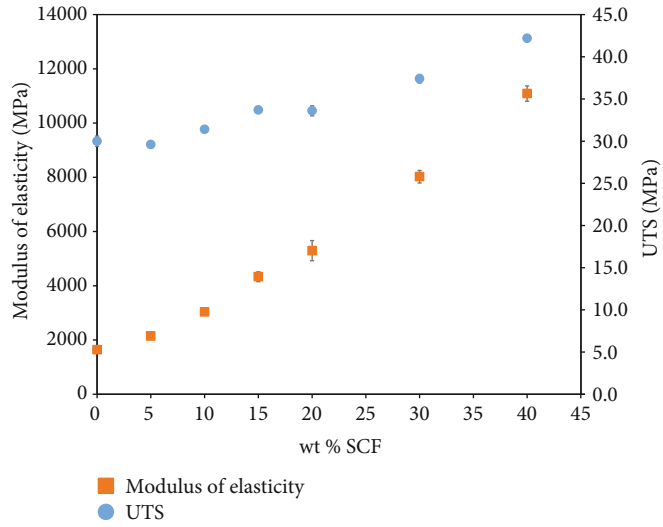

Figure 3: Modulus of elasticity and UTS for different wt% of SCF (0–40 wt% of SCF).

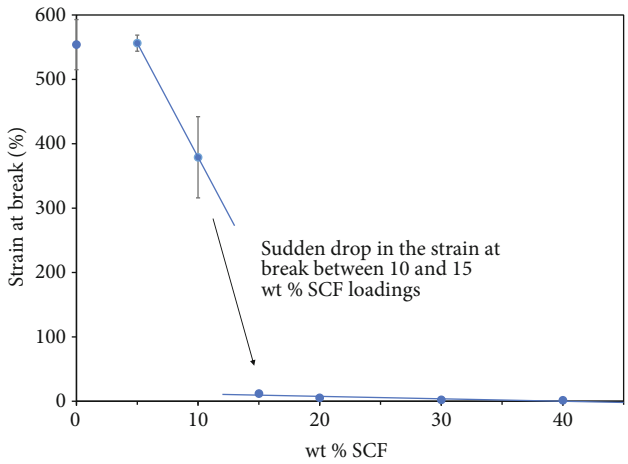

Figure 4: Strain at break of the PP/SCF composite with 0–40 wt% of SCF.

matrix disturbs matrix continuity, which results in the premature failure of the material. A similar behavior was observed in composites with 30 wt% and 40 wt% of SCF loading, where plastic deformation was almost not observed.

From the stress-strain curves, the mechanical properties of neat PP and PP/SCF composites with varying percentages of SCF were obtained, and the corresponding values are shown in Table 4. Figure 3 shows the composites' experimental results of the modulus of elasticity and UTS with an increase in wt% of SCF; meanwhile, Figure 4 shows the composite strain at break with an increase in wt% of SCF. Figure 3 shows that the modulus of elasticity and UTS of the composite increased with an increase in SCF loading. The presence of SCF in PP increases the modulus of elasticity because SCF inhibits the movement of the PP molecule chain. The inhibition of the PP molecular chain alignment is known to increase with an increase in the concentration of SCF loading in the PP matrix; thus, the modulus of elasticity increased by up to 575% in the composite with 40-wt% SCF loading. However, it was observed that an increase in UTS was not as pronounced as an increase in the modulus of elasticity. At 40-wt% SCF loadings, the tensile strength increased by only 40%. The tensile strength of the PP/SCF composite is affected by fiber length and interfacial bonding between the fiber and matrix [22]. The average length of fibers used in this study was 150 μm. Thus, it can be predicted that the composites

Table 5: Mechanical properties of neat PP and its composites with 10–15 wt% of SCF.

Tag name	wt% SCF	Strain at break (%)
PP/10SCF	10	379 ± 48
PP/11SCF	11	261 ± 63
PP/12SCF	12	152 ± 89
PP/13SCF	13	156 ± 153
PP/14SCF	14	17 ± 1.5
PP/15SCF	15	12 ± 2.5

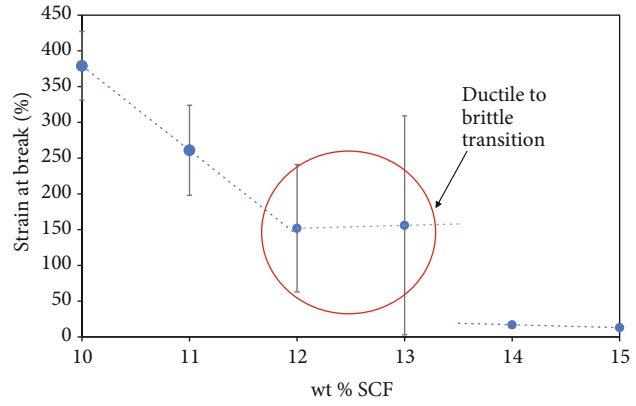

Figure 5: Strain at break of the PP/SCF composite with 10–15 wt% of SCF.

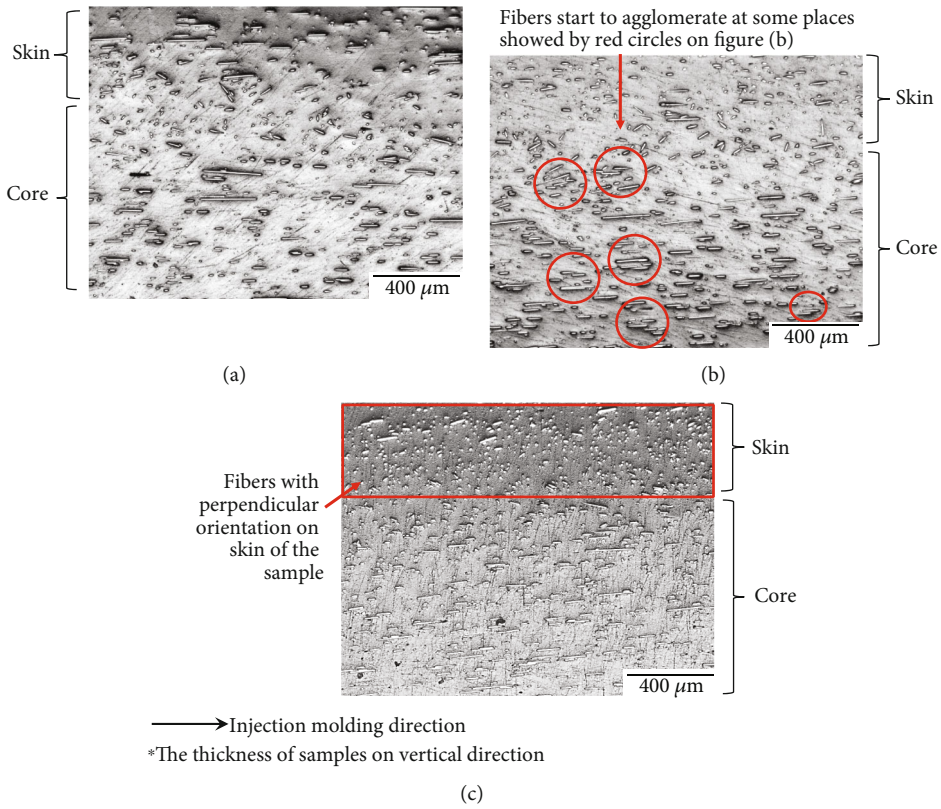

Figure 6: OM images of longitudinal section of (a) 10 wt%, (b) 13 wt%, and (c) 15 wt% of SCF.

prepared in this investigation will exhibit lower interfacial bonding between the fibers and PP matrix. On the other hand, it was observed that the strain at break or the ductility of processed composites decreased with an increase in the wt% loading of SCF. A closer look at the decreasing trend of ductility values revealed that the decreasing trend started to appear in the composites with greater than 5 wt% SCF loading. No considerable changes were observed in composites with 5 wt% or less of SCF. In addition, a considerable decrease in ductility values was observed when the concentration of SCF was 10–15 wt%. The ductility decreased from 379% strain in the composite with 10 wt% of SCF to 12% strain in the composite with 15 wt% of SCF, as shown in Figure 4. The considerable and sudden decrease in ductility was determined to be dependent on the specific concentration regime of SCF. This regime can be considered the ductility transformation regime in which the composite showed ductile behavior at lower concentrations and brittle behavior at higher concentrations.

To further investigate the transformation regime, four additional composites were prepared with 10–15 wt% of SCF, and tensile experiments were conducted to obtain the strain at break (ductility) values of these composites. The values of strain at break for these composites are shown in Table 5. The experimental results clearly show that the strain at break of composites linearly decreases up to 11 wt% of SCF; then, in the range of 12–13 wt% of SCF, fluctuations appeared in the strain at break values, followed by the considerable (sudden) decrease in strain in composites that contained 14 wt% of SCF. The strain at break for these composites was determined to be 17% (shown in Figure 5). Thus, it can be clearly deduced that the presence of 12–13 wt% of SCF in reinforced composites results in the ductile to brittle transition of composites processed in this study.

3.2. Microstructures. To further understand the failure mechanism of the processed composites, microstructural investigations were performed. The microstructure of the composites obtained using an optical microscope (OM) is shown in Figure 6. This figure clearly shows that the distribution of SCF has random orientation; some fibers were aligned along the direction of injection; other fibers were aligned perpendicular, and few were aligned at an angle with the injection direction. It is also observed that some fibers were broken during the manufacturing process. This is attributed to the fiber to machine and fiber to fiber interactions that occur during the manufacturing process [23]. The addition of fibers along with an increase in the number of fibers (as a result of broken fibers) will create more fiber ends. In addition, the number of fiber ends tends to increase with an increase in SCF concentration. These fiber ends and fibers with perpendicular direction with tension loading will likely be the failure path. Figure 6(a) shows that fibers are almost evenly distributed on the PP matrix for the PP/10SCF composite, and less agglomeration is observed. For PP/13SCF, as shown in Figure 6(b), it was observed that SCFs in the PP matrix started to approach each other; at some locations, this started to create more agglomeration as marked by red

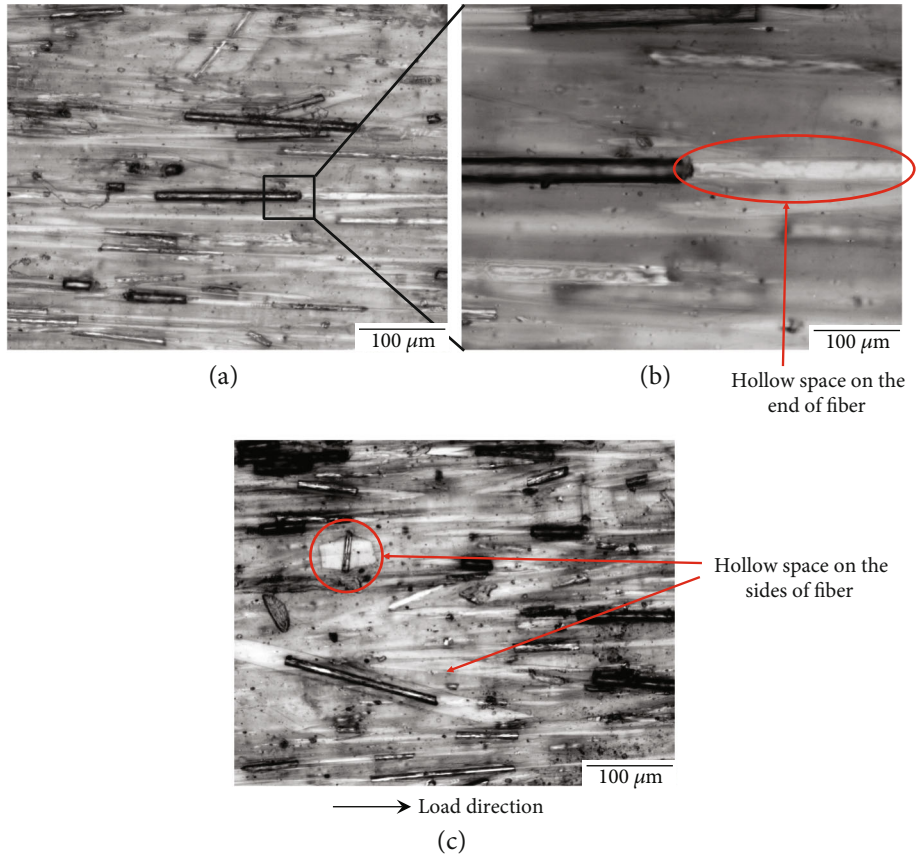

Figure 7: OM images of PP/10SCF composite surface microstructure after the tensile test. (a) SCF perpendicular to the load direction. (b) Image in (a) at higher magnification. (c) SCF misaligned to the load direction.

circles. In addition, these fiber agglomerations can create stress concentration that may be responsible for a decrease in the strain at break. Meanwhile, for the PP/15SCF composite, more fibers are oriented perpendicular to the injection molding direction on the skin region of the sample, as shown in Figure 6(c) by the red rectangle area.

3.3. Fracture Surface. The microstructure of the PP/10SCF composite after the tensile experiment is obtained using an optical microscope as shown in Figure 7. PP/10SCF experiences a very high strain, i.e., up to 379%. The microstructure in Figure 7(a) shows a hollow space on the ends of fibers owing to the elongation of the matrix during the tensile loading. The creation of hollow space is due to the difference in the nature of materials. The matrix is ductile with low strength, and SCF is brittle with a several folds higher strength than that of the matrix. In addition, the interfacial shear stress between the fiber and matrix is usually not sufficient to induce fiber fracture. The lower interfacial stress may be attributed to the length of the fiber, which in this study was less than the critical length needed for inducing a substantially higher interfacial bonding strength. The critical fiber length is defined as the minimum length of the fiber where the load transmitted from the matrix to the fiber is maximum [24]. Fu et al. [23] have calculated the critical fiber length between PP (as the matrix) and CF to be more than 800 μm. Thus, the creation of hollow space at the end of the

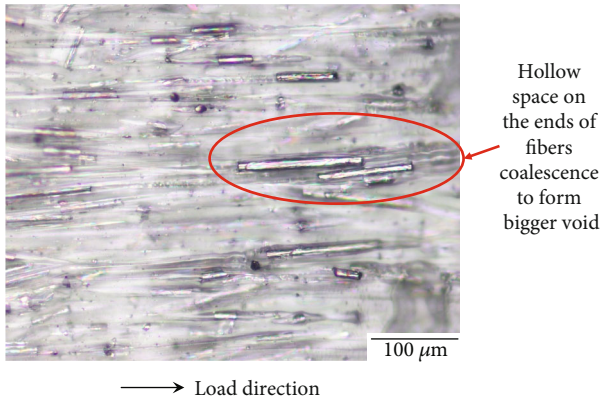

Figure 8: OM image of PP/15SCF composite surface microstructure after the tensile test.

fibers and lower interfacial strength resulted in the lower strain at break (ductility) values. Figure 7(c) shows the microstructure of PP/10SCF with some fibers misaligned to the force direction. The orientation of fibers at an angle to the loading direction results in the creation of larger voids on both sides of the fiber, as shown by the circle in Figure 7(c). However, because the distance between different fibers was sufficient, the failure did not occur on this site. Figure 8 reveals the microstructure of the PP/15SCF composite after the tensile experiment. For the PP/15SCF composite,

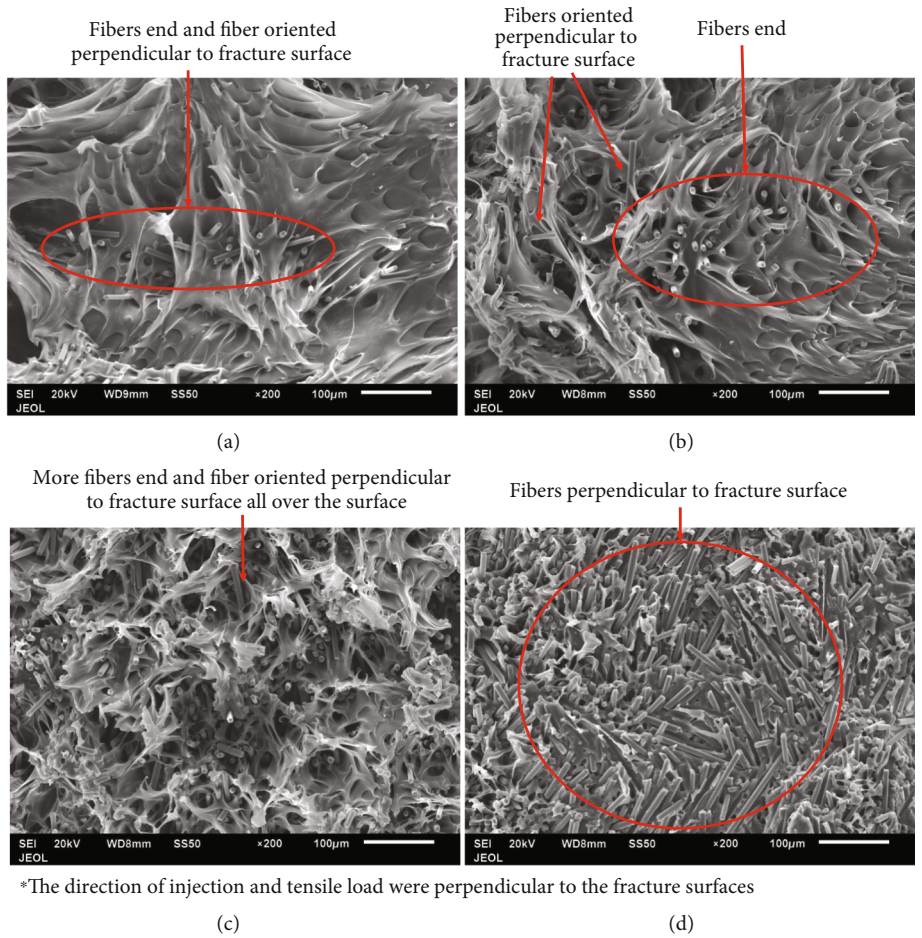

Figure 9: SEM images of tensile fracture surface for (a) PP/15SCF, (b) PP/20SCF, (c) PP/30SCF, and (d) PP/40SCF composites.

the distance between fibers decreases; thus, during the tensile test, hollow spaces, which form during elongation, can coalesce with each other to form bigger microvoids.

The fracture mechanism of polymer-reinforced short fibers with random orientation during the tensile test has been previously studied by Sato et al. [25, 26]. They proposed that failure starts at the interface between fiber ends and fiber sides, which initiates cracks. Failure starts at the interface between fiber ends when fibers are parallel to the stress direction; failure starts at fiber sides when fibers are aligned perpendicular to the stress direction. An increase in the wt% of SCF will increase the number of fiber ends and increases the number of SCF which are oriented perpendicular to the loading direction. In addition, the distance between fibers will decrease, which will lead to faster crack propagation. An increase in the wt% of SCF will decrease the ability of the polymer to elongate before fracture. The combination of fiber ends and fiber sides misaligned in the loading direction may be responsible for the fracture mechanism observed in the composites.

Figure 9 shows the tensile fracture surface of PP/SCF composites used in this study. The loading direction and injection molding direction were perpendicular to the fracture surface. The fracture surface for PP/15SCF, PP/20SCF, and PP/30SCF exhibits a dimpled fracture, which starts from

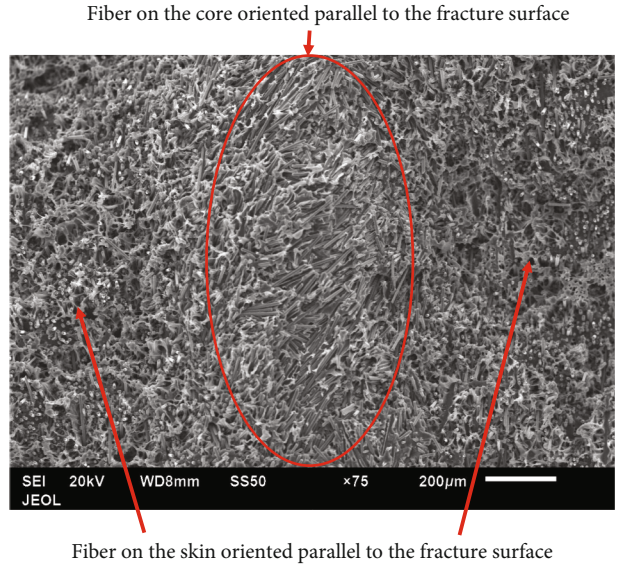

Figure 10: SEM image of tensile fracture surface PP/40SCF at low magnification (loading and injection molding direction perpendicular to the fracture surface).

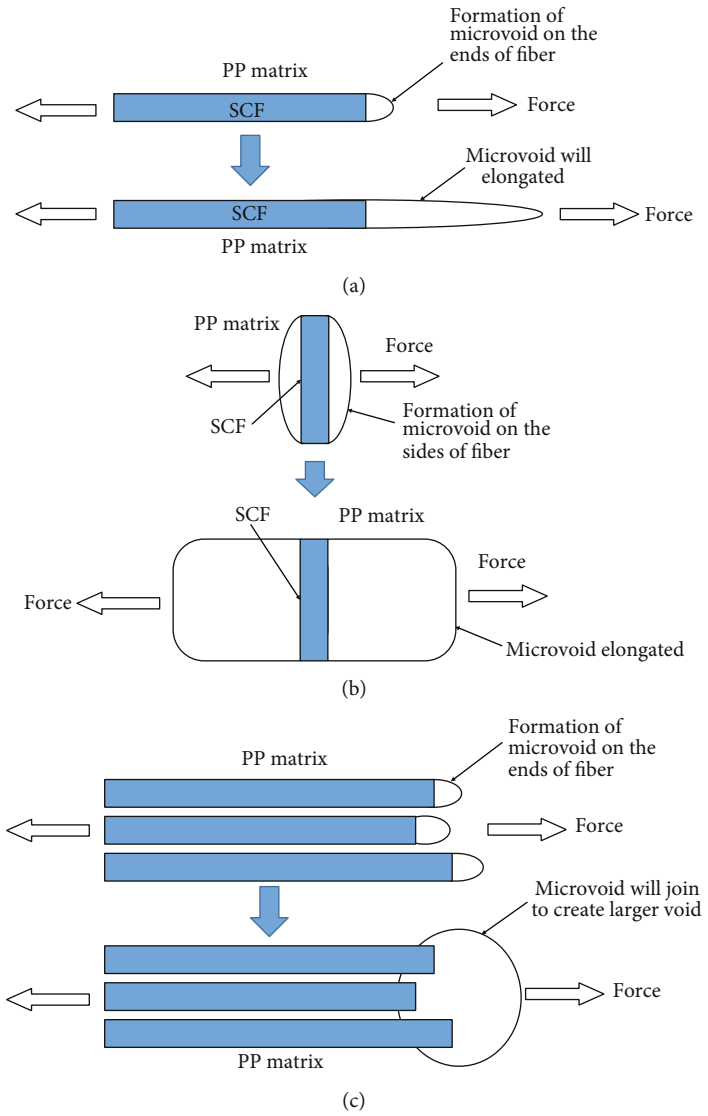

Figure 11: Formation of microvoids on (a) single SCF oriented parallel to the force, (b) single SCF oriented perpendicular to the force, and (c) agglomerate SCF oriented parallel to the force.

either the end of the fiber or the fiber misaligned to the loading direction. The dimpled structure is created from the microvoid, which is formed during the elongation of the composite. In addition, it is known that SCF has very low ductility, whereas the PP matrix exhibits high ductility, and their composites tend to have weak interfacial bonding. All of these factors result in the formation of microvoids in the composites. Microvoids are formed at the end of the fiber when fibers are oriented parallel to the force and at the side of the fiber when fibers are oriented at an angle to the applied forces. Figure 9(d) shows the fracture surface of the PP/40SCF composite. The micrograph shows some areas with fibers perpendicular to the loading direction.

A lower magnification image of the PP/40SCF composite is shown in Figure 10. This figure shows that at the core or middle part of the composite, fibers tend to orient perpendicular to injection direction; while on the outer sides, fibers tend to orient parallel to the injection molding direction.

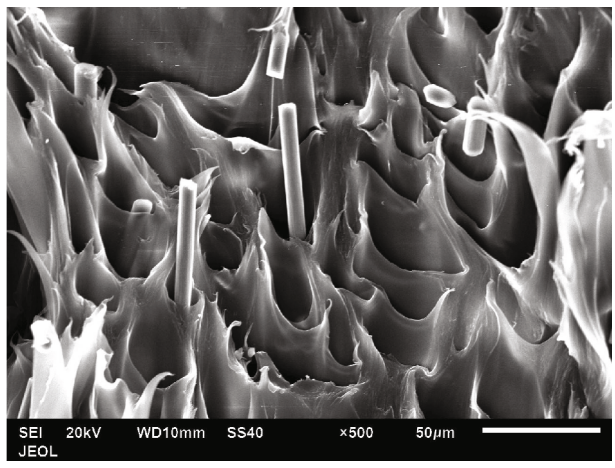

Figure 12: SEM image of fracture surface for the PP/13SCF composite (loading direction perpendicular to the fracture surface).

These core parts of the PP/40SCF composite constitute the most possible sites where failure starts to occur. The occurrence of core and skin structures on the fiber-reinforced composite has been previously reported [27–29]. At low loading (PP/10SCF), microvoids continue to elongate with an increase in the elongation of the composites, as shown in Figures 11(a) and 11(b). Meanwhile, at the higher loading of SCF, the distance between adjacent fiber ends becomes shorter, and the higher the loading is, the closer the fiber ends are. Under continuous loading, the microvoids at the ends of each fiber will coalesce to form bigger voids; this will eventually lead to the failure of composites at relatively low strain values. This mechanism is shown in Figure 11(c). This mechanism is probably the reason why the tensile fracture surfaces still show the occurrence of some plastic deformation before the fracture occurs even at high loading of fillers.

Figure 12 shows the fracture surface for the additional composition for the PP/13SCF composite with low strain at break. The force direction is perpendicular to the surface. The PP/13SCF composite exhibits a fluctuation number for strain at break. The figure shows that the fibers were oriented perpendicular to the dimple fracture surface. An increase in the wt% of SCF also leads to an increase in the presence of fibers oriented perpendicular to the direction of the applied force. This may be the source for the formation of microvoids that eventually end in the failure of the composite, as is shown earlier in Figure 11(b). Smaller microvoids will coalescence with each other to form larger voids, which will lead to the fracture of the composite.

4. Conclusions

In this study, the PP/SCF composite samples were prepared with different wt% SCF loading (i.e., 0, 5, 10, 15, 20, 30, and 40 wt%) followed by 4 additional compositions (i.e., 11, 12, 13, and 14 wt%). The mechanical properties of the samples were investigated through tensile tests. The results showed that the modulus of elasticity and the tensile strength of PP/SCF composites increased with an increase in the wt% of SCF. Compared with neat PP, the modulus and tensile strength (of 40-wt% SCF loaded composite) increased by 574.9% and 40.7%, respectively. In addition, the strain at break decreased to 17% strain for PP/14SCF (14-wt% SCF) compared to 553% strain for neat PP. The ductile to brittle transition in the composite appeared in the range of 12–13-wt% loading of SCF. Microscopic examination showed that SCFs tended to agglomerate at 13-wt% SCF loadings. The SEM images of the fracture surface indicated that fiber ends and fibers oriented perpendicular to the loading direction were responsible for the failure of the composite.

Data Availability

The experimental data used to support the findings of this study may be released upon application/personal request to the first author, who can be contacted at hjunaedi@ksu.edu.sa.

Conflicts of Interest

The authors declare that there is no conflict of interest regarding the publication of this paper.

Acknowledgments

The authors would like to thank Deanship of Scientific Research at King Saud University, Saudi Arabia, for funding and supporting this research through the initiative of DSR Graduate Student Research Support (GSR).

References

[1] J. Jansz, "Polypropylene in automotive applications," in *Polypropylene: An A-Z Reference*, J. Karger-Kocsis, Ed., pp. 643–651, Springer Netherlands, Dordrecht, 1999.

[2] R. J. Tapper, M. L. Longana, H. Yu, I. Hamerton, and K. D. Potter, "Development of a closed-loop recycling process for discontinuous carbon fibre polypropylene composites," *Composites Part B: Engineering*, vol. 146, pp. 222–231, 2018.

[3] M. Holmes, "Recycled carbon fiber composites become a reality," *Reinforced Plastics*, vol. 62, no. 3, pp. 148–153, 2018.

[4] T. Gallone and A. Zeni-Guido, "Closed-loop polypropylene, an opportunity for the automotive sector," *The Journal of Field Actions*, no. 19, pp. 48–53, 2019.

[5] J. G. Poulakis, P. C. Varelidis, and C. D. Papaspyrides, "Recycling of polypropylene-based composites," *Advances in Polymer Technology*, vol. 16, no. 4, 322 pages, 1997.

[6] Automated Dynamic, "Short-Fiber Reinforced," August 2020, http://www.automateddynamics.com/article/thermoplastic-composite-basics/types-of-thermoplastic-composites/short-fiber-reinforcement.

[7] S. J. Park, *Carbon Fibers*, Springer Singapore, 2018.

[8] N. G. Karsli and A. Aytac, "Effects of maleated polypropylene on the morphology, thermal and mechanical properties of short carbon fiber reinforced polypropylene composites," *Materials and Design*, vol. 32, no. 7, pp. 4069–4073, 2011.

[9] H. Junaedi, A. Alfawzan, S. Aloraini, T. Almutairi, and A. Almajid, "Mechanical, physical, and wear properties of polypropylene reinforced short carbon fiber composites with different fiber length," in *21st International Conference on Composite Materials*, Xi'an, China, 2017.

[10] H. Junaedi, E. Albahkali, M. Baig, and A. Almajid, "The effect compatibilizer on mechanical properties of short carbon fiber reinforced polypropylene composites," *AIP Conference Proceedings*, vol. 1981, article 020028, 2018.

[11] C. Ozkan, N. Gamze Karsli, A. Aytac, and V. Deniz, "Short carbon fiber reinforced polycarbonate composites: effects of different sizing materials," *Composites Part B: Engineering*, vol. 62, pp. 230–235, 2014.

[12] D. Pérez-Rocha, A. B. Morales-Cepeda, F. Navarro-Pardo, T. Lozano-Ramírez, and P. G. LaFleur, "Carbon fiber composites of pure polypropylene and maleated polypropylene blends obtained from injection and compression moulding," *International Journal of Polymer Science*, vol. 2015, Article ID 493206, 8 pages, 2015.

[13] C.-L. Huang, C.-W. Lou, C.-F. Liu, C.-H. Huang, X.-M. Song, and J.-H. Lin, "Polypropylene/graphene and polypropylene/carbon fiber conductive composites: mechanical, Crystallization

and Electromagnetic Properties," *Applied Sciences*, vol. 5, no. 4, pp. 1196–1210, 2015.

[14] J. Karger-Kocsis and K. Friedrich, "Fracture behavior of injection-molded short and long glass fiber-polyamide 6.6 composites," *Composites Science and Technology*, vol. 32, no. 4, pp. 293–325, 1988.

[15] Y. Xiaochun, Y. Youhua, F. Yanhong, Z. Guizhen, and W. Jinsong, "Preparation and characterization of carbon fiber/polypropylene composites via a tri-screw in-line compounding and injection molding," *Advances in Polymer Technology*, vol. 37, no. 8, 3872 pages, 2018.

[16] H. Uematsu, Y. Suzuki, Y. Iemoto, and S. Tanoue, "Effect of maleic anhydride-grafted polypropylene on the flow orientation of short glass fiber in molten polypropylene and on tensile properties of composites," *Advances in Polymer Technology*, vol. 37, no. 6, 1763 pages, 2018.

[17] W. N. Ota, S. C. Amico, and K. G. Satyanarayana, "Studies on the combined effect of injection temperature and fiber content on the properties of polypropylene-glass fiber composites," *Composites Science and Technology*, vol. 65, no. 6, pp. 873–881, 2005.

[18] N. G. Karsli and A. Aytac, "Tensile and thermomechanical properties of short carbon fiber reinforced polyamide 6 composites," *Composites Part B: Engineering*, vol. 51, pp. 270–275, 2013.

[19] U.S. Congress, Office of Technology Assessment, *Advanced Materials by Design*, Government Printing Office, Washington, DC: U.S., 1988.

[20] ASTM D638-14, "Standard Test Method for Tensile Properties of Plastics," ASTM International, West Conshohocken, PA, 2014, https://www.astm.org/.

[21] W. D. Callister and D. G. Rethwisch, *Materials Science and Engineering: An Introduction*, Wiley, 8th edition, 2009.

[22] P. K. Mallick, *Composites Engineering Handbook*, Marcel Dekker, Inc, New York, 1997.

[23] S. Y. Fu, B. Lauke, E. Mäder, C. Y. Yue, and X. Hu, "Tensile properties of short-glass-fiber- and short-carbon-fiber-reinforced polypropylene composites," *Composites Part A: Applied Science and Manufacturing*, vol. 31, no. 10, pp. 1117–1125, 2000.

[24] V. G. Geethamma, R. Joseph, and S. Thomas, "Short coir fiber-reinforced natural rubber composites: effects of fiber length, orientation, and alkali treatment," *Journal of Applied Polymer Science*, vol. 55, no. 4, pp. 583–594, 1995.

[25] N. Sato, T. Kurauchi, S. Sato, and O. Kamigaito, "Mechanism of fracture of short glass fibre-reinforced polyamide thermoplastic," *Journal of Materials Science*, vol. 19, no. 4, pp. 1145–1152, 1984.

[26] N. Sato, T. Kurauchi, S. Sato, and O. Kamigaito, "Microfailure behaviour of randomly dispersed short fibre reinforced thermoplastic composites obtained by direct SEM observation," *Journal of Materials Science*, vol. 26, no. 14, pp. 3891–3898, 1991.

[27] X. Yan and S. Cao, "Structure and interfacial shear strength of polypropylene-glass fiber/carbon fiber hybrid composites fabricated by direct fiber feeding injection molding," *Composite Structures*, vol. 185, pp. 362–372, 2018.

[28] X. Yan, P. Uawongsuwan, M. Murakami, A. Imajo, Y. Yang, and H. Hamada, "Tensile properties of glass fiber/carbon fiber reinforced polypropylene hybrid composites fabricated by direct fiber feeding injection molding process," in *ASME International Mechanical Engineering Congress and Exposition*, vol. 2, Advanced Manufacturing: V002T02A45, 2016.

[29] S. Y. Fu, B. Lauke, and Y.-W. Mai, *Science and Engineering of Short Fibre Reinforced Polymer Composites*, Woodhead Publishing Limited, Cambrige, UK, 2009.